A Thesis

entitled

Verification and Validation Method for an Acoustic Mode Prediction Code for Turbomachinery Noise

by

Jeffrey Severino

Submitted to the Graduate Faculty as partial fulfillment of the requirements for the Masters of Science Degree in Mechanical Engineering

Dr. Ray Hixon, Committee Chair

Dr. Chinhua Sheng, Committee Member

Dr. Soric Cioc, Committee Member

Dr. Patricia R. Komuniecki, Dean
College of Graduate Studies

The University of Toledo
- 2022

An Abstract of

Verification and Validation Method for
an Acoustic Mode Prediction Code for Turbomachinery Noise

by

Jeffrey Severino

Submitted to the Graduate Faculty as partial fulfillment of the requirements for the Masters of Science Degree in Mechanical Engineering

The University of Toledo
- 2022

Over the last 20 years, there has been an increase in computational fluid dynamic codes that have made numerical analysis more and more readily available, allowing turbomachine designers to create more novel designs. However, as airport noise limitations become more restrictive over time, reducing aircraft takeoff and landing noise remains a prominent issue in the aviation community. One popular method to reduce aircraft noise is using acoustic liners placed on the walls of the engine inlet and exhaust ducts. These liners are designed to reduce the amplitude of acoustic modes emanating from the bypass fan as they propagate through the engine. The SWIRL code is a frequency-domain linearized Euler equation solver that is designed to predict the effect of acoustic liners on acoustic modes propagating in realistic sheared and swirling mean flows, guiding the design of more efficient liner configurations. The purpose of this study is to validate SWIRL using the Method Of Manufactured Solutions (MMS). This study also investigated the effect of the integration and spatial differencing methods on the convergence for a given Manufactured Solution. In addition, the effect of boundary condition implementation was tested. The improved MMS convergence rates shown for these tests suggest that the revised SWIRL code provides more accurate solutions with less computational effort than the original formulation.

Acknowledgments

This work is supported by the NASa Advanced Air Transport Technologies (AATT) Project. I would like to thank Edmane Envia of the NASA Glenn Research Center, who is the technical monitor of this work. A very special thanks goes to Dr. Ray Hixon who supervised and guided me through out my course work and Master's Thesis. His rigor and tenacity in his profession has been the model example for an aspiring aeroacoustician. I would like to also thank all of my committee members, Dr. Chunhua Sheng and Dr. Sorin Cioc. Their contributions have been instrumental. Thanks to Dr. Clifford Brown for his programatic insights.

I would also like to thank my focus group peers, Zaid Sabri, Matthew Gibbons , and Gabriel Gutierrez for their patience and support over the years. I wish them the best in all of their endevours.

Contents

List of Tables

List of Figures

List of Symbols

A ..... mean flow speed of sound
A_T ..... speed of sound at the duct radius
$\tilde{A}$ ..... dimensionless speed of sound, $\frac{A}{A_T}$
D/Dt ..... material derivative, $\partial/\partial t + V \cdot \nabla$
D_N ..... derivative matrix using N points
$\mathbf{e}_x$,$\mathbf{e}_\theta$ ..... unit vectors for the axial and tangential directions
k_x ..... perturbation axial wavenumber
k ..... reduced frequency, $\omega r_{max}/A_T$
m ..... number of nodal diameters, i.e. azimuthal mode number
M_x ..... axial Mach number
M_θ ..... tangential Mach number
P ..... mean pressure
p' ..... perturbation pressure
r ..... radial coordinate
r_{min} ..... hub radius, i.e. minimum radius
r_{max} ..... hub radius, i.e. maximum radius
$\bar{r}$ ..... dimensionless radial coordinate, r/r_{max}
$\bar{r}_{Shankar}$ .... dimensionless radial coordinate in **??** , $r/b = r/(r_{max} - r_{min})$
S ..... mean entropy
s' ..... perturbation entropy
t ..... time
$\vec{V}$ ..... mean flow velocity vector
v ..... mean flow velocity
v' ..... perturbation flow velocity
v_x ..... axial component of mean flow velocity
v_θ ..... tangential component of mean flow velocity
v'_r ..... axial component of perturbation velocity
v'_x ..... axial component of perturbation velocity
v'_θ ..... tangential component of perturbation flow velocity
v_ϕ ..... phase velocity,$k/\bar{\gamma}$
v_g ..... group velocity,$dk/d\bar{\gamma}$
x ..... axial coordinate

Greek Symbols

$\bar{\gamma}$ ..... dimensionless axial wavenumber, $k_x r_{max}$
Γ ..... free vortex strength
$\bar{\Gamma}$ ..... $\Gamma/(r_T A_T)$
δ ..... Kronecker delta
η_H ..... hub acoustic liner admittance (at r_{min})
η_T ..... tip acoustic liner admittance (at r_{max})
Θ ..... circumferential/azimuthal coordinate
κ ..... ratio of specific heats
$\kappa_{m\mu}$ ..... modal separation constant
λ ..... eigenvalue, $-i\bar{\gamma}$
μ ..... radial mode index
$\bar{\rho}$ ..... mean density
ρ' ..... perturbation density
σ ..... hub-to-tip radius ratio, r_{min}/r_{max}
Ω ..... angular frequency for solid body swirl
$\bar{\Omega}$ ..... $\Omega r_T/A_T$
ω ..... perturbation angular frequency

List of Abbreviations

CAA	Computational Aeroacoustics
CFD	Computational Fluid Dynamics
MMS	Method of Manufactured Solutions
TSM	Tanh Summation Method
NS	Navier-Stokes
RK	Runge-Kutta

Preface

Chapter 1

Theoretical Framework and Methods

1.1 Introduction

This chapter will outline the steady and unsteady aerodynamic models used for this study. The MMS procedure as it is used in this study will be described. The summation method used to generate symbolic expression will be breifly described. This chapter will also present the use of fairing functions to impose the equivallent boundary conditions used in the numerical approximation. The procedure for calculating the approximated rate of convergence for a system of equations is also presented.

1.2 Governing Equations for Compressible, Inviscid Flow

The governing equations for an isentropic, inviscid, compressible gas with density, ρ, velocity, $\vec{V}$, and pressure, p describe the conservation of mass, momentum, and energy for a given domain in Equations (1.1, 1.2, 1.2) respectively.

$$\frac{D\rho}{Dt} = -\rho\nabla\cdot\vec{V} \tag{1.1}$$

$$\frac{D\vec{V}}{Dt} = -\frac{\nabla p}{\rho} + \vec{g} \tag{1.2}$$

$$\frac{Ds}{Dt} = 0 \tag{1.3}$$

where D/Dt is the material derivative operator,,

$$\frac{D}{Dt} = \frac{\partial}{\partial t} + \nabla\cdot\vec{V} \tag{1.4}$$

For this model, the domain is assumed to be uniformly cylindrical. Therefore the flow is assumed to be asymmetric, then the radial velocity component is zero. With this considered, the velocity vector ,$\vec{V}$ in cylindrical coordinates become,

$$\vec{V}(r,\theta,x) = v_x(r)\hat{e}_x + v_\theta(r)\hat{e}_\theta \tag{1.5}$$

where $\hat{e}_x$ and $\hat{e}_\theta$ are unit vectors for the axial and tangential directions.The gradient operator ,∇ in cylindrical coordinates, is

$$\vec{\nabla} = \hat{e}_r\frac{\partial}{\partial r} + \frac{1}{r}\hat{e}_\theta\frac{\partial}{\partial\theta} + \frac{\partial}{\partial z}\hat{e}_z = 0 \tag{1.6}$$

To close the problem and to write in terms of pressure, the thermodynamic relation for the speed of sound is used

$$A^2 = \frac{\partial p}{\partial\rho}\Big|_s \tag{1.7}$$

Utilizing the equation of state in differential form and with material derivatives

$$\frac{Dp}{Dt} = A^2 \frac{D\rho}{Dt} + \frac{\partial p}{\partial s}\Big|_\rho \frac{Ds}{Dt} \tag{1.8}$$

The convervation of energy can be rewritten in terms of pressure, by using 1.7 and 1.8

$$\frac{Dp}{Dt} = A^2 \frac{D\rho}{Dt}. \tag{1.9}$$

Using the 1.1 in non-conservative form and the definition $A^2 = \gamma p/\rho$ (See Appendix for derivation)

$$\frac{Dp}{Dt} + \gamma p \left(\nabla \cdot \vec{V}\right) = 0. \tag{1.10}$$

Expanding equations (1.1, 1.2, 1.10) with the corresponding cylindrical expressions become,

$$\frac{\partial \rho}{\partial t} + v_r \frac{\partial \rho}{\partial r} + \frac{v_\theta}{r}\frac{\partial \rho}{\partial \theta} + v_x \frac{\partial \rho}{\partial \theta} + \rho\left(\frac{1}{r}\frac{\partial (r v_r)}{\partial r} + \frac{1}{r}\frac{\partial v_\theta}{\partial \theta} + \frac{\partial v_x}{\partial x}\right) = 0 \tag{1.11}$$

$$\frac{\partial v_r}{\partial t} + v_r \frac{\partial v_r}{\partial r} + \frac{v_\theta}{r}\frac{\partial v_r}{\partial \theta} - \frac{v_\theta^2}{r} + v_x \frac{\partial v_r}{\partial x} = -\frac{1}{\rho}\frac{\partial p}{\partial r} \tag{1.12}$$

$$\frac{\partial v_\theta}{\partial t} + v_r \frac{\partial v_\theta}{\partial r} + \frac{v_\theta}{r}\frac{\partial v_\theta}{\partial \theta} + \frac{v_r v_\theta}{r} + v_x \frac{\partial v_\theta}{\partial x} = -\frac{1}{\rho r}\frac{\partial p}{\partial \theta} \tag{1.13}$$

$$\frac{\partial v_x}{\partial t} + v_r \frac{\partial v_x}{\partial r} + \frac{v_\theta}{r}\frac{\partial v_x}{\partial \theta} + v_x \frac{\partial v_x}{\partial x} = -\frac{1}{\rho}\frac{\partial p}{\partial x} \tag{1.14}$$

$$\frac{\partial p}{\partial t} + v_r \frac{\partial p}{\partial r} + \frac{v_\theta}{r}\frac{\partial p}{\partial \theta} + v_x \frac{\partial p}{\partial \theta} + \gamma p\left(\frac{1}{r}\frac{\partial (r v_r)}{\partial r} + \frac{1}{r}\frac{v_\theta}{\partial \theta} + \frac{\partial v_x}{\partial x}\right) = 0 \tag{1.15}$$

1.3 Nonuniformities from swirling mean flow

If the mean flow contains a swirling component, i.e. a velocity vector in the tangential direction, the mean quantities, pressure , density are non-uniform, thus also changing the speed of sound. By integrating the radial momentum equation, an expression for the speed of sound was established to account for the resulting

nonuniformities due to rotations in the flow.

$$p = \int_{r_{min}}^{r_{max}} \frac{\rho v_\theta^2}{r} dr \tag{1.16}$$

where r_{min} and r_{max} are the bounds of the radius. Since the flow is isentropic, the pressure is related to the speed of sound through $\nabla p = A^2 \nabla \rho$; which is used to compute ρ. With the relationship $A^2 = \gamma p/\rho$, the speed of sound is found to be,

$$\tilde{A}(\tilde{r}) = exp\left[\left(\frac{1-\gamma}{2}\right)\int_{\tilde{r}}^{1} \frac{M_\theta}{\tilde{r}} \partial \tilde{r}\right] \tag{1.17}$$

The appendix shows how the speed of sound was extracted. For special cases of swirling flow, the relation to between the speed of sound and the tangential velocity can be found. Expressions can be derived for free vortex , and/or solid body swirl. The non-dimesionalization is shown in the next section.

1.4 Linearizing the Governing Equations

To linearize the Euler equations, we substitute each flow variable with its equivalent mean and perturbation components. Note that the mean term is only a function of space whereas the perturbation component is a dependent on both space and time (functional dependence is not explicity written with each variable). Assuming that we can divide the variable into a known laminar flow solution to the governing equations and a small amplitude perturbation solution,

$$v_r = V_r(x) + v_r' \tag{1.18}$$

$$v_\theta = V_\theta + v_\theta' \tag{1.19}$$

$$v_x = V_x + v_x' \tag{1.20}$$

$$p = \bar{p} + p' \tag{1.21}$$

$$\rho = \bar{\rho} + \rho' \tag{1.22}$$

One key assumption is that the perturbation quantites, $\tilde{p}$, $\tilde{v}_r$,$\tilde{v}_\theta$, and $\tilde{v}_x$, are all exponential and that they are solely a function of radius,

$$v_r' = v_r(r)e^{i(k_x x + m\theta - \omega t)} \tag{1.23}$$

$$v_\theta' = v_\theta(r)e^{i(k_x x + m\theta - \omega t)} \tag{1.24}$$

$$v_x' = v_x(r)e^{i(k_x x + m\theta - \omega t)} \tag{1.25}$$

$$p' = p(r)e^{i(k_x x + m\theta - \omega t)} \tag{1.26}$$

There are a few important assumptions that will be utilized,

- The small disturbances are infinitesimal (thus linearized)
- Neglect second order terms.
- The continuity equation is comprised of mean velocity components. This is subtracted off in each of the governing equations

The following relationships were utlized to simplify the linearized equations,

$$\frac{\partial P}{\partial r} = \frac{\bar{\rho} V_\theta^2}{r}$$

$$\gamma P = \bar{\rho} A^2$$

$$\rho' = \frac{1}{A^2} p'$$

Note that the momentum equation in the θ and x directions remain unchanged. The term $\frac{\partial (r v_r')}{\partial r} = \frac{\partial (r)}{\partial r} v_r' + \frac{\partial v_r'}{\partial r} r$ in the Energy equation

$$\frac{1}{\bar{\rho} A^2} \left(\frac{\partial p'}{\partial t} + \frac{V_\theta}{r} \frac{\partial p'}{\partial \theta} + V_x \frac{\partial p'}{\partial x} \right) + \frac{V_\theta^2}{A^2 r} v_r' + \frac{\partial v_r'}{\partial r} + \frac{v_r'}{r} + \frac{1}{r} \frac{\partial v_\theta'}{\partial \theta} + \frac{\partial v_x'}{\partial x} = 0$$

$$\frac{\partial v_r'}{\partial t} + \frac{V_\theta}{r} \frac{\partial v_r'}{\partial \theta} - \frac{2 V_\theta v_\theta'}{r} + V_x \frac{\partial v_r'}{\partial x} = \frac{1}{\bar{\rho}} \frac{\partial p'}{\partial r} + \frac{V_\theta}{\bar{\rho} r A^2} p'$$

$$\frac{\partial v_\theta'}{\partial t} + v_r' \frac{\partial V_\theta}{\partial r} + \frac{V_\theta}{r} \frac{\partial v_\theta'}{\partial \theta} + \frac{v_r' V_\theta}{r} + V_x \frac{\partial v_\theta'}{\partial x} = -\frac{1}{\bar{\rho} r} \frac{\partial p'}{\partial \theta}$$

$$\frac{\partial v_x'}{\partial t} + v_r' \frac{\partial V_x}{\partial r} + \frac{V_\theta}{r} \frac{\partial v_x'}{\partial \theta} + V_x \frac{\partial v_x'}{\partial x} = -\frac{1}{\bar{\rho}} \frac{\partial p'}{\partial x}$$

Substituting Equation (1.26) into the linearized equations will give us the final governing equations.

$$i \left(-\omega + \frac{m}{r} + k_x V_x \right) v_r - \frac{2 \bar{v_\theta}}{r} v_\theta = -\frac{1}{\bar{\rho}} \frac{\partial P}{\partial r} + \frac{V_{\theta^2}}{A^2} \frac{1}{\bar{\rho} r} p$$

$$i \left(-\omega + \frac{m}{r} + k_x V_x \right) v_\theta + \left(\frac{V_\theta}{r} + \frac{\partial V_\theta}{\partial r} \right) v_\theta = -\frac{m}{\bar{\rho} r} p$$

$$i \left(-\omega + \frac{m V_\theta}{r} + k_x V x \right) v_x + \frac{\partial V_x}{\partial r} v_r = -\frac{i k_x}{\bar{\rho}} p$$

$$\frac{1}{\bar{\rho} A^2} \left(-i\omega + \frac{i m V_\theta}{r} + i k_x V_x + \right) p(r) + \frac{V_\theta^2}{A^2 r} v_r + \frac{v_r}{r} + \frac{\partial v_r(r)}{\partial r} + \frac{i m}{r} v_\theta(r) + i k_x v_x(r) = 0$$

1.5 Non-Dimensionalization

Defining

$$r_T = r_{max}$$

$$A_T = A(r_{max})$$

$$k = \frac{\omega r_T}{A_T}$$

$$\bar{\gamma} = k_x r_T$$

$$\tilde{r} = \frac{r}{r_T}$$

$$\frac{\partial}{\partial r} = \frac{\partial \tilde{r}}{\partial r}\frac{\partial}{\partial \tilde{r}} = \frac{1}{r_T}\frac{\partial}{\partial \tilde{r}}$$

$$V_\theta = M_\theta A$$

$$V_x = M_x A$$

$$\tilde{A} = \frac{A}{A_T}$$

$$v_x = \tilde{v}_x A$$

$$v_r = \tilde{v}_r A$$

$$v_\theta = \tilde{v}_\theta A$$

$$p = \tilde{p}\bar{\rho}A^2$$

Substituting in yields ,

$$i\left[-\frac{k}{\tilde{A}} + \frac{mM_\theta}{\tilde{r}} + \bar{\gamma}M_x\right]\tilde{v}_r - \frac{2M_\theta \tilde{v}_\theta}{\tilde{r}} = -\frac{\partial \tilde{p}}{\partial \tilde{r}} - (\gamma - 1)\frac{\gamma M_\theta}{\tilde{r}}\tilde{p} \quad (1.27)$$

$$i\left[-\frac{k}{\tilde{A}} + \frac{mM_\theta}{\tilde{r}} + \bar{\gamma}M_x\right]\tilde{v}_\theta + \left(\frac{M_\theta}{\tilde{r}} + \frac{1}{A}\frac{\partial M_\theta A}{\partial \tilde{r}}\right)\tilde{v}_r = \frac{im}{\tilde{r}}\tilde{p} \quad (1.28)$$

$$i\left[-\frac{k}{\tilde{A}} + \frac{mM_\theta}{\tilde{r}} + \bar{\gamma}M_x\right]\tilde{v}_x + \frac{1}{A}\frac{\partial M_x A}{\partial \tilde{r}}\tilde{v}_r = -i\bar{\gamma}\tilde{p} \quad (1.29)$$

$$i\left[-\frac{k}{\tilde{A}} + \frac{mM_\theta}{\tilde{r}} + \bar{\gamma}M_x\right]\tilde{p} + \frac{M_\theta^2}{\tilde{r}}\tilde{v}_r + \frac{\partial \tilde{v}_r}{\partial \tilde{r}} + \frac{1}{A}\frac{\partial A}{\partial \tilde{r}}v_r + \frac{\tilde{v}_r}{\tilde{r}} + \frac{im}{\tilde{r}}\tilde{v}_\theta + i\bar{\gamma}\tilde{v}_x = 0 \quad (1.30)$$

Defining, $\lambda = -i\bar{\gamma}$

and defining

$$\{\bar{x}\} = \begin{Bmatrix} \tilde{v}_r \\ \tilde{v}_\theta \\ \tilde{v}_x \\ \tilde{p} \end{Bmatrix}$$

The governing equations can be written in the form of $[A]x - \lambda[B]x$

$$\begin{bmatrix} -i\left(\frac{k}{\tilde{A}} - \frac{mM_\theta}{\tilde{r}}\right) - \lambda M_x & -\frac{2M_\theta}{\tilde{r}} & 0 & \frac{\partial}{\partial \tilde{r}} + \frac{\gamma-1}{\tilde{r}} \\ \frac{M_\theta}{\tilde{r}} + \frac{\partial M_\theta}{\partial \tilde{r}} + \left(\frac{\gamma-1}{2}\right)\frac{M_\theta^3}{\tilde{r}} & -i\left(\frac{k}{\tilde{A}} - \frac{mM_\theta}{\tilde{r}}\right) - \lambda M_x & 0 & \frac{im}{\tilde{r}} \\ \frac{\partial M_x}{\partial \tilde{r}} + \left(\frac{\gamma-1}{2}\frac{M_x M_\theta^2}{\tilde{r}}\right) & 0 & -i\left(\frac{k}{\tilde{A}} - \frac{mM_\theta}{\tilde{r}}\right) - \lambda M_x & -\lambda \\ \frac{\partial}{\partial \tilde{r}} + \frac{\gamma+1}{2}\frac{M_\theta^2}{\tilde{r}} + \frac{1}{\tilde{r}} & \frac{im}{\tilde{r}} & -\lambda & -i\left(\frac{k}{\tilde{A}} - \frac{mM_\theta}{\tilde{r}}\right) - \lambda M_x \end{bmatrix} \bar{x} = 0$$

1.6 Analytical Solution to Sound Propagation in ducted flows

$$\frac{1}{A^2}\left(\frac{\partial^2 p}{\partial t^2}\right) - \left(\frac{\partial^2 p}{\partial t^2} + \frac{1}{\tilde{r}}\frac{\partial p}{\partial r} + \frac{1}{\tilde{r}^2}\frac{\partial^2 p}{\partial \theta^2} + \frac{\partial^2 p}{\partial x^2}\right) = 0$$

The method of separation of variables requires an assumed solution as well as initial and boundary conditions. For a partial differential equation, the assumed solution can be a linear combination of solutions to a system of ordinary differential equations that comprises the partial differential equation. Since p is a function of four variables, the solution is assumed to be a linear combination of four solutions. Each solution is assumed to be Euler's identity, a common ansant for linear partial differential equations and boundary conditions.

Defining,

$$p(x, r, \theta, t) = X(x)R(r)\Theta(\theta)T(t) \tag{1.31}$$

where,

$$X(x) = A_1 e^{ik_x x} + B_1 e^{-ik_x x}$$

$$\Theta(\theta) = A_2 e^{ik_\theta \theta} + B_2 e^{-ik_\theta \theta}$$

$$T(t) = A_3 e^{i\omega t} + B_3 e^{-i\omega t}$$

The next step is to rewrite the wave equation in terms of X, R, Θ, and T. To further simplify the result, each term is divided by p.

$$\frac{1}{A^2}\frac{1}{T}\frac{\partial^2 T}{\partial t^2} = \frac{1}{R}\frac{\partial^2 R}{\partial r^2} + \frac{1}{r}\frac{1}{R}\frac{\partial R}{\partial r} + \frac{1}{r^2}\frac{1}{\Theta}\frac{\partial \Theta}{\partial \theta} + \frac{1}{X}\frac{\partial^2 X}{\partial x^2} \tag{1.32}$$

Notice that each term is only a function of its associated independent variable. So, if we vary the time, only the term on the left-hand side can vary. However, since none of the terms on the right-hand side depend on time, that means the right-hand side cannot vary, which means that the ratio of time with its second derivative is independent of time. The practical upshot is that each of these terms is constant, which has been shown. The wave numbers are the *separation constants* that allow the PDE to be split into four separate ODE's. Substituting the separation constants into Equation (1.32) gives,

$$\frac{1}{R}\left(\frac{\partial^2 R}{\partial r^2} + \frac{1}{r}\frac{\partial R}{\partial r}\right) - \frac{k_\theta^2}{r^2} - k_x^2 + k^2 = 0 \tag{1.33}$$

The remaining terms are manipulated to follow the same form as *Bessel's Differntial Equation* ,

The general solution to Bessel's differential equation is a linear combination of the Bessel functions of the first kind, $J_n(k_r r)$ and of the second kind, $Y_n(k_r r)$ [1]. The subscript n refers to the order of Bessel's equation.

$$R(r) = (AJ_n(k_r r) + BY_n(k_r r)) \tag{1.34}$$

where the coefficients A and B are found after applying radial boundary conditions.

By rearranging Equation (1.33), a comparison can be made to Equation (**??**) to show that the two equations are of the same form.

The first step is to revisit the radial derivatives that have not been addressed. As was done for the other derivative terms, the radial derivatives will also be set equal to a separation constant, $-k_r^2$.

$$\underbrace{\frac{1}{R}\left(\frac{\partial^2 R}{\partial r^2} + \frac{1}{r}\frac{\partial R}{\partial r}\right) - \frac{k_\theta^2}{r^2}}_{-k_r^2} - k_x^2 + k^2 = 0 \tag{1.35}$$

Following the same procedure, the axial wavenumber is,

$$\begin{aligned} k_x &= \frac{2M_x k \pm \sqrt{4M_x^2 k^2 + 4\beta^2\left(k^2 - k_r^2\right)}}{-2\beta^2} \\ &= \frac{-M_x k \pm \sqrt{k^2 - k_r^2}}{\beta^2} \end{aligned}$$

Chapter 2

Results and Discusssion

2.1 Verification

2.1.1 Introduction

The frequency domain, linearized Euler equation computer code, SWIRL, was verified through the Methods of Manufactured and Exact solutions. However, while the Method of Exact Solutions (MES) can be used to validate the ouput of SWIRL, there is a limitation on the number of exact solutions available based on the flow and domain. Any changes in a flow configuration (uniform axial flow vs. sheared axial flow, without any tangential component) require a recalculation of the analytical solution. Code validation through MES is for the case of uniform flow in a cylindrical duct since the exact solution requires implementing special Bessel functions . In addition, the exact solution needs to be recomputed for changes in radii and the use of acoustic liner (i.e., boundary conditions). For this reason, the more comprehensive MMS was first used for code verification to test each variable in the governing equations and gain measurable acceptance criteria without relying on expert judgment.

MMS was implemented on a component level since SWIRL consists of two main numerical approximations for flows with axial and tangential components. First, the numerical integration technique required for radial change in sound speed was

verified. Then, the four governing equations that make up the matrices required for the eigenvalue problem were tested. Note that the output of the eigenvalue problem was tested with MMS by recomputing the expression $[A]x - \lambda[B]x = 0$ with a given eigenvalue/vector pair. The calculated $L_{2,norm}$ (i.e. error and the order of accuracy for both numerical methods are discussed below. The MMS was then used to compare against validation cases in literature to outline the methodolody for test cases for which there is no solution.

2.1.2 MMS, Solutions

(insert table instead of equations, check comments in tex file for parameters)

$$M_x = 0.3\left(\sum_{j=1}^{5} R_{ij} + \sum_{j=1}^{5} L_{ij} + 1\right), B = 50 \tag{2.1}$$

$$\tilde{A} = \left(\sum_{j=1}^{5} R_{ij} + \sum_{j=1}^{5} L_{ij} + 1\right), B = 0.3 \tag{2.2}$$

$$\tilde{v}_{r,BCsImposed} = \sum_{j=1}^{3} R_{ij} + \sum_{j=1}^{3} L_{ij} + 1, \tag{2.3}$$

$$B = 2, \tag{2.4}$$

$$\tilde{v}_{r,BCsImposed}(\tilde{r}_{min} = \tilde{r}_{max}) = 0 \tag{2.5}$$

$$\tilde{v}_{\theta} = \left(\sum_{j=1}^{4} R_{ij} + \sum_{j=1}^{4} L_{ij} + 1\right), B = 50 \tag{2.6}$$

$$\tilde{v}_{x} = \sum_{j=1}^{3} R_{ij} + \sum_{j=1}^{3} L_{ij} + 1, B = 30 \tag{2.7}$$

$$\tilde{p}_{diffBCsImposed} = \sum_{j=1}^{5} R_{ij} + \sum_{j=1}^{5} L_{ij} + 1, B = 30 \tag{2.8}$$

Figure 2-1 shows the manufactured solution for the mean flow profile. The tangent summation method was used to generate the axial Mach number, the speed of sound, and the perturbation variables. The tangential Mach number was numerically approximated by using the composite trapezoidal rule. The manufactured mean flow profile is unique because it has been generated solely to verify SWIRL and does not have physical significance. The "kinks" in the solution will allow a significant magnitude for the derivatives of these solutions.

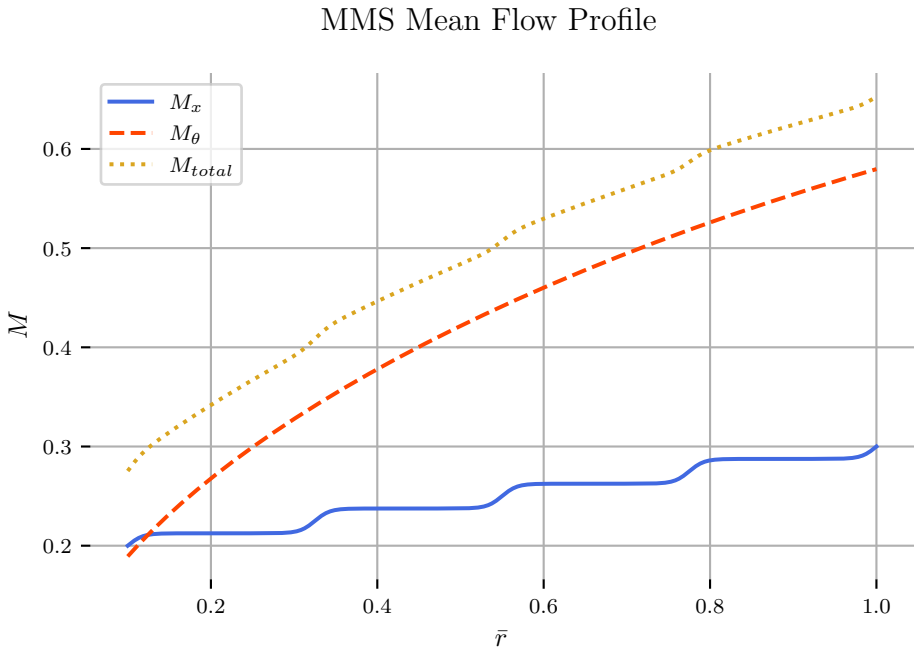

Figure 2-1: The manufactured mean flow test case using a summation of Tangents for A and M_x

The results from the numerical integration are presented in Figure 2-2. Although the slope of the line appears linear, the TSM was still used to generate the MS for the speed of sound. Denser grids were used to compute the error by iterating as grid

spacing approaches zero. The difference between the expected speed of sound to the actual speed of sound is shown in Figure 2-3 as a function of radius. Note that the error reaches machine precision early in the iterations and approaches zero as more grid points are used.

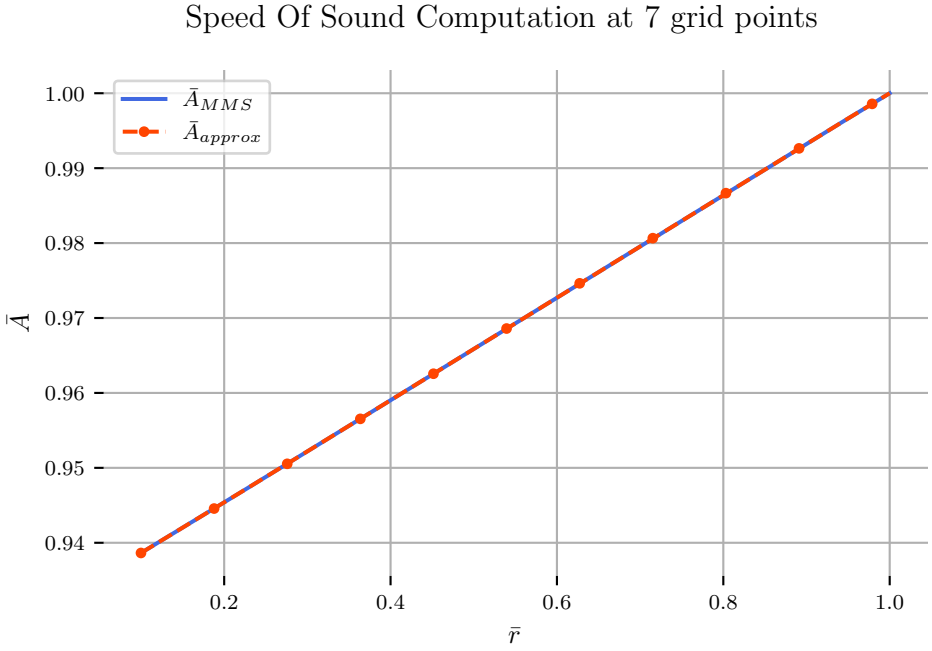

Figure 2-2: A comparison of the speed of sound, expected vs actual at the lowest grid to show similarities in solution

The error will decrease at a known rate depending on the type of numerical integration scheme. Since the composite trapezoidal rule has an order of accuracy of 2, it is expected that the approximated order of accuracy will approach two as the error approaches zero. This behavior is shown in Figure 2-4, where the approximated line is the L2 norm of the speed of sound error. The slope (i.e., the asymptotic rate of convergence) approached two for numerical integration as the grid spacing decreases (See Figure 2.1.2) .

The manufactured solution used for the fluctuation variables in the MMS test case is shown in Table **??**. Recall that the variable B varies the slope around the tangent

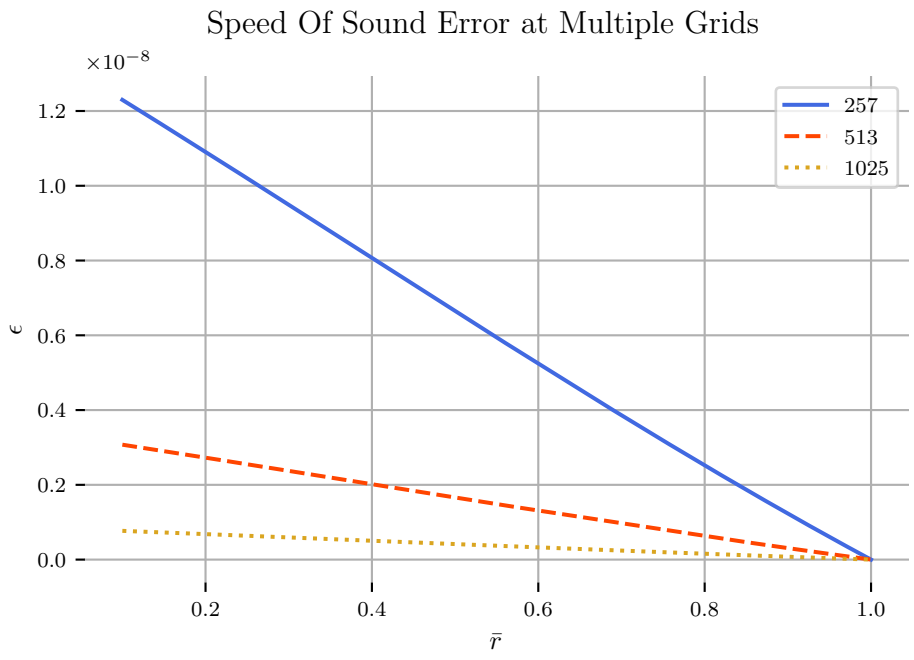

Figure 2-3: A comparison of the speed of sound error at three grid

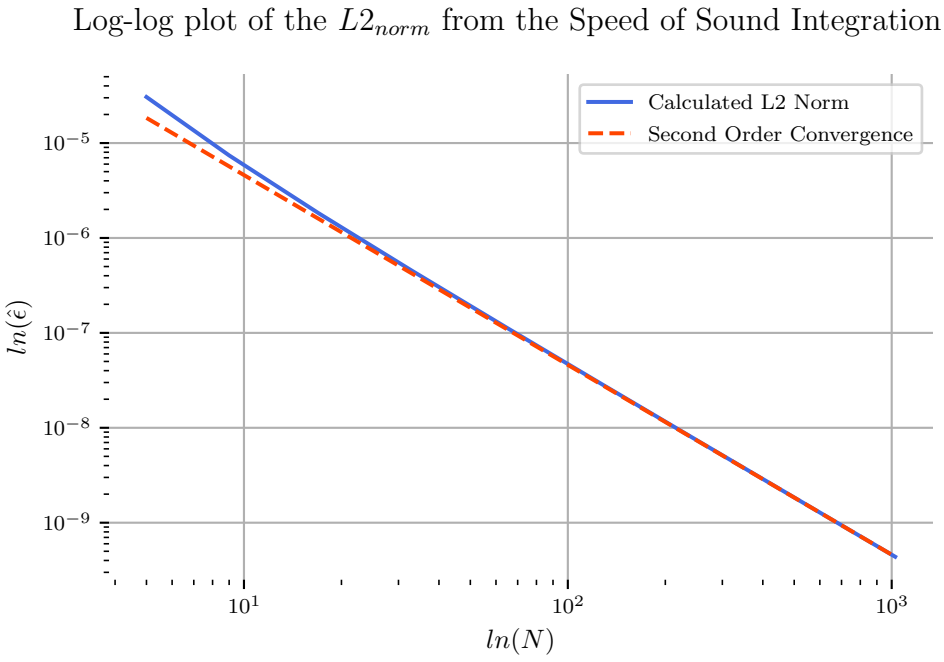

Figure 2-4: L2 Norm comparison for the speed of sound integration for the compound trapezoidal rule

function at each inflection point; the maximum amplitude of each tangent function was A = 0.1 and was equally spaced between $\tilde{r}_{min}$-$\tilde{r}_{max}$. The boundary conditions for the perturbation variable $\tilde{v}_r$ were set using the fairing functions to impose boundary conditions. Fairing functions also set the derivative of the perturbation variable $\tilde{p}$. Only $\tilde{p}$ is affected by acoustic liners since it alters the rate of change of pressure at the walls, not the pressure or velocity. The subscripts $BCsImposed, diffBCsImposed$ state where the perturbation or its derivative value was altered to be uniform between the code and the manufactured solution.

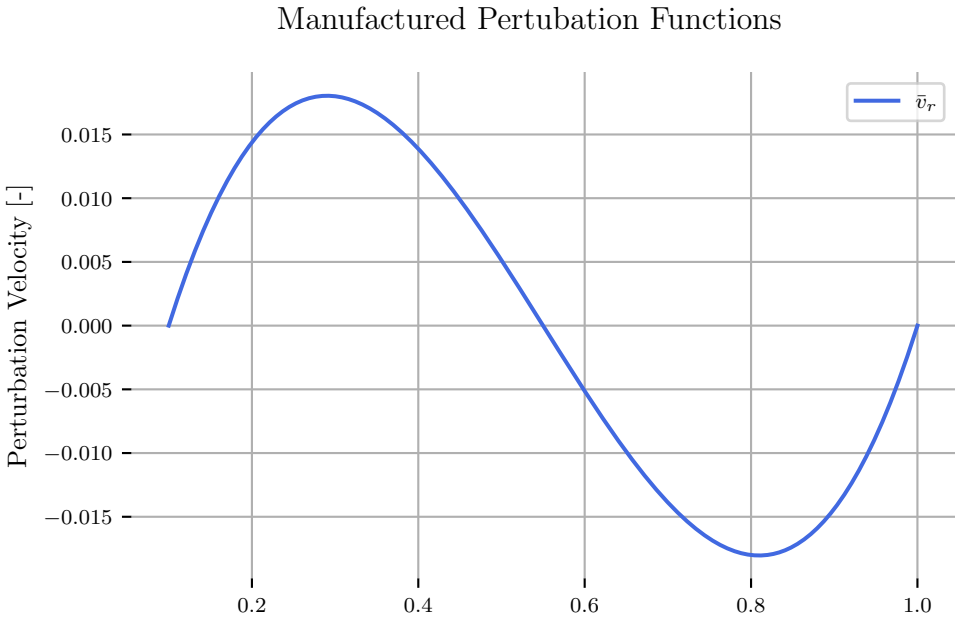

Figure 2-5: The manufactured perturbation functions ,v_r

A second and fourth-order central differencing scheme for the LEE is used for the approximated radial derivatives and compared to the source terms generated for the MMS in Figure 5-10.The L2 norm and the asymptotic rate of convergence is shown for the two diffferencing schemes in 5-15 .

The grid points were doubled, starting at 7 grid points and ending after 9 iterations with 1025 grid points. Both schemes do not have the order of accuracy down to

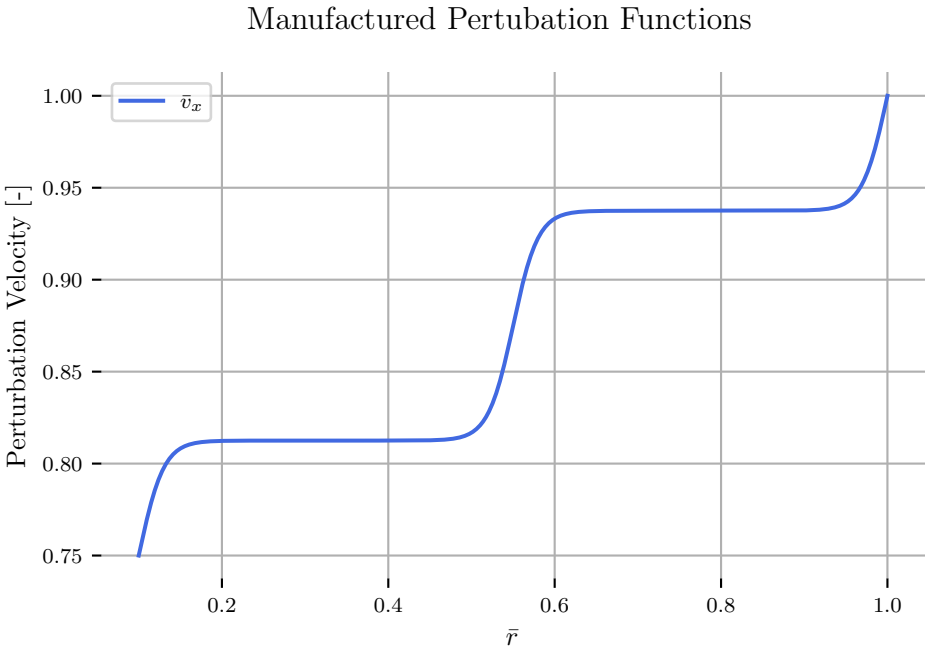

Figure 2-6: The manufactured perturbation functions ,v_x

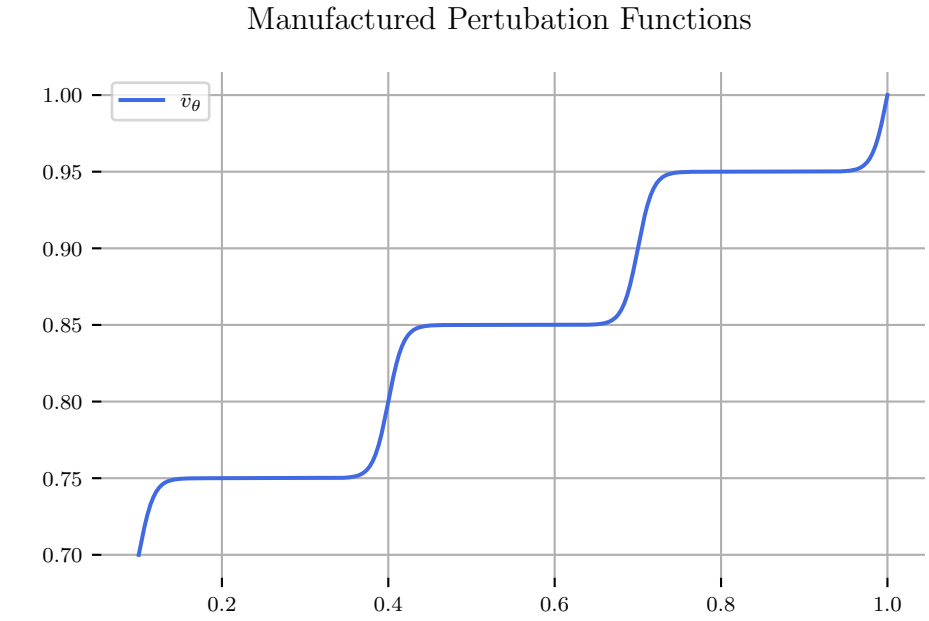

Figure 2-7: The manufactured perturbation functions ,v_θ

machine precision but get down to $10^{-}6$ For the LEE, a second and fourth order central differencing scheme is used for the approximated radial derivatives and then

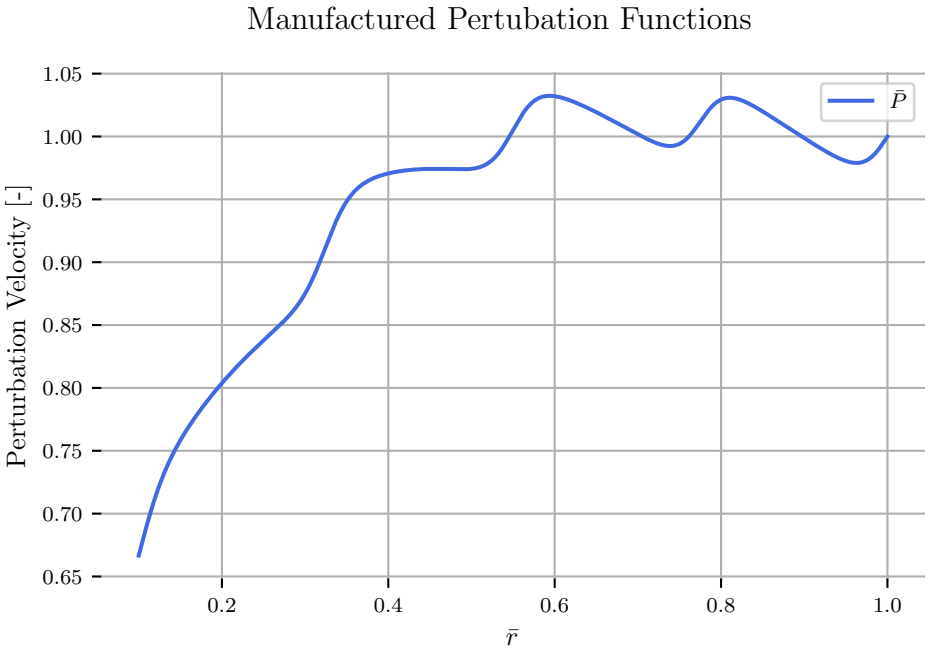

Figure 2-8: The manufactured perturbation functions ,P

compared to the source terms generated for the MMS in Figure 2-10.

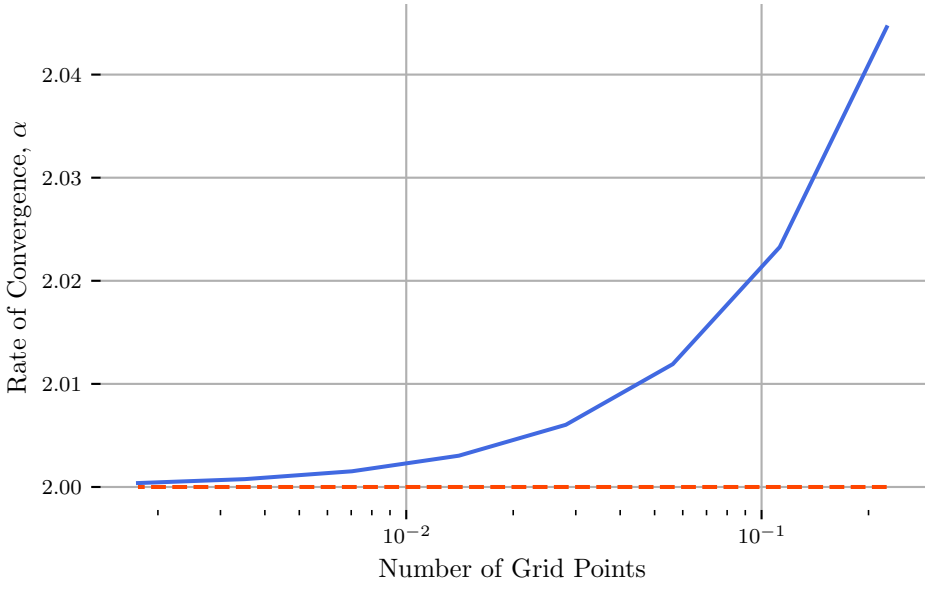

Figure 2-9: Speed of Sound Rate Of Convergence

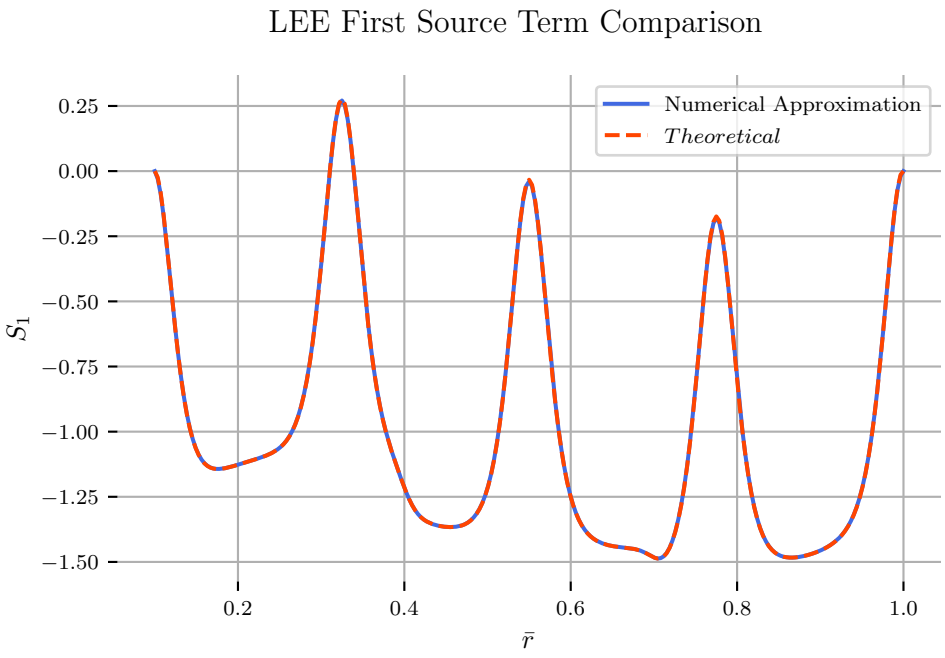

Figure 2-10: LEE Source Terms

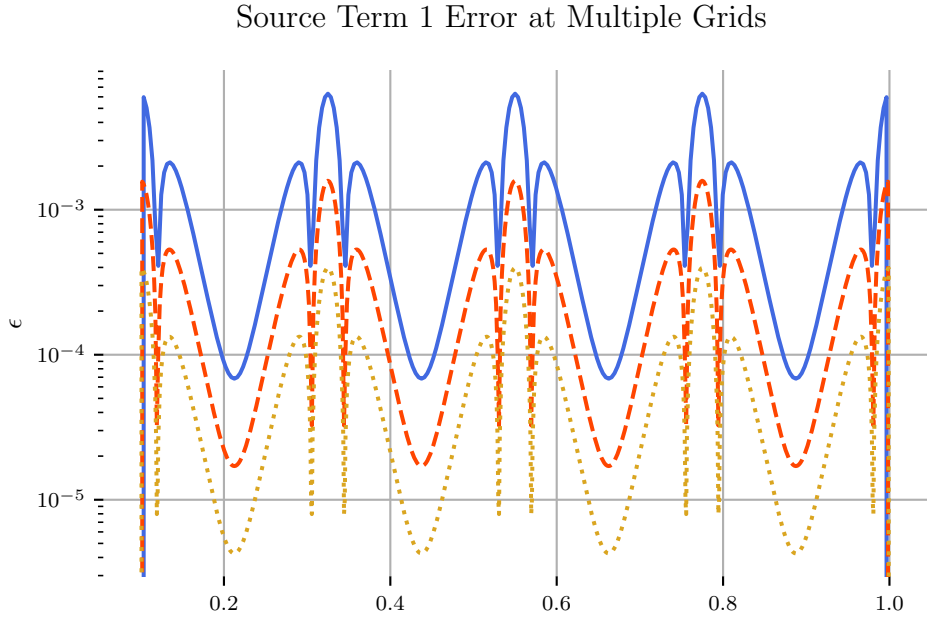

Figure 2-11: LEE Source Term Error

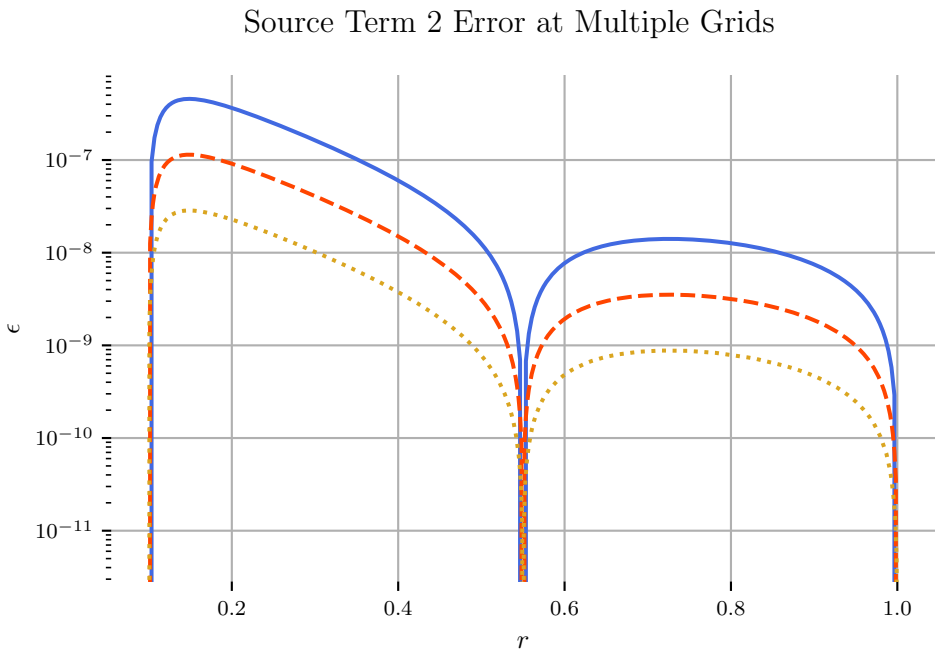

Figure 2-12: LEE Source Term Error

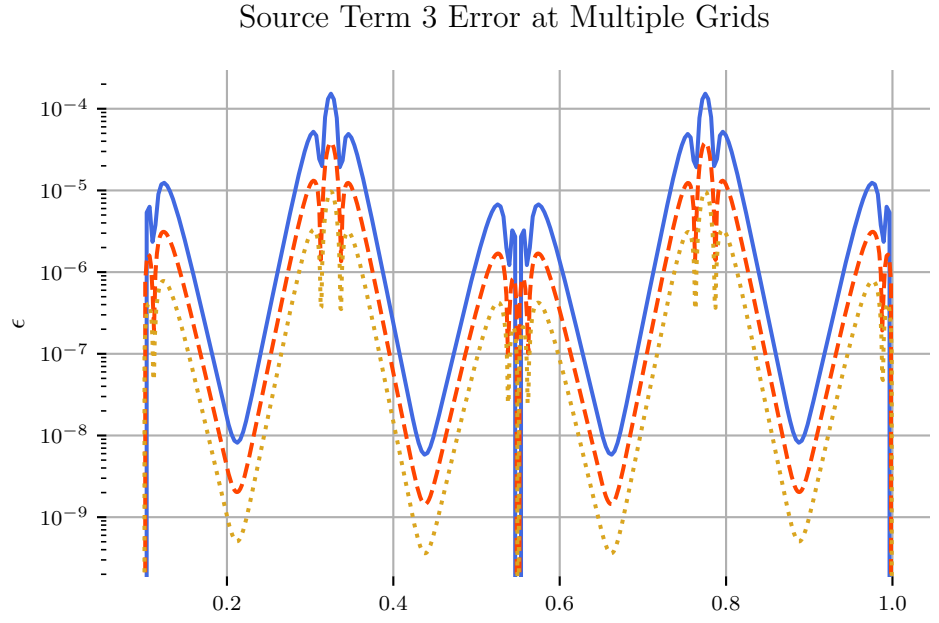

Figure 2-13: LEE Source Term Error

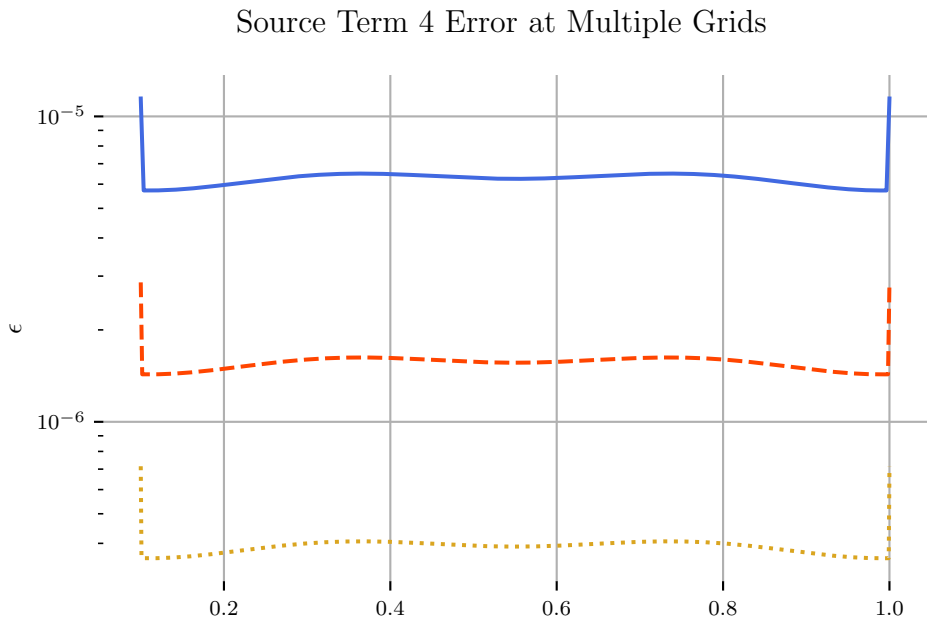

Figure 2-14: LEE Source Term Error

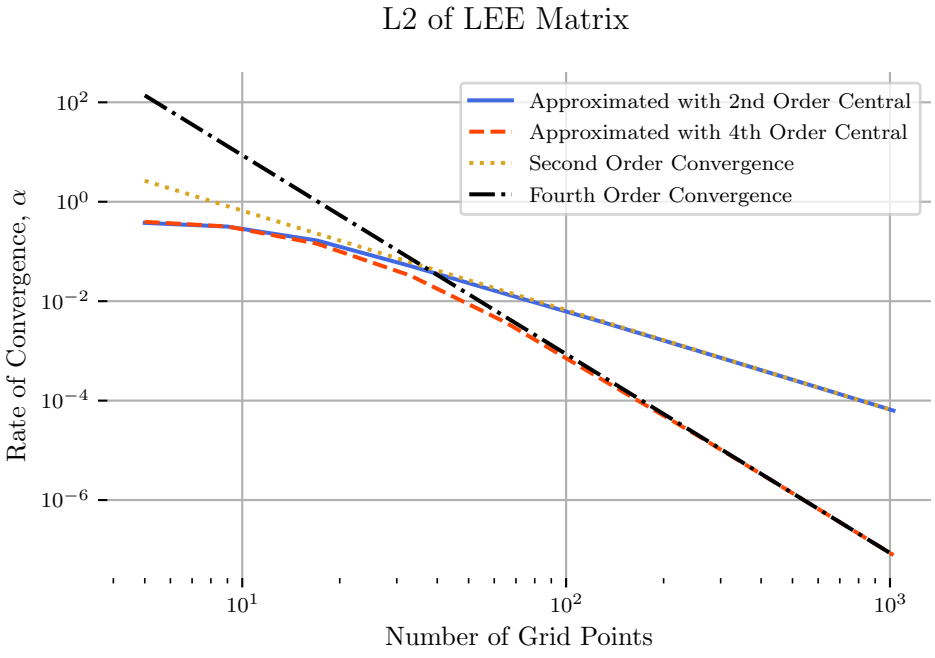

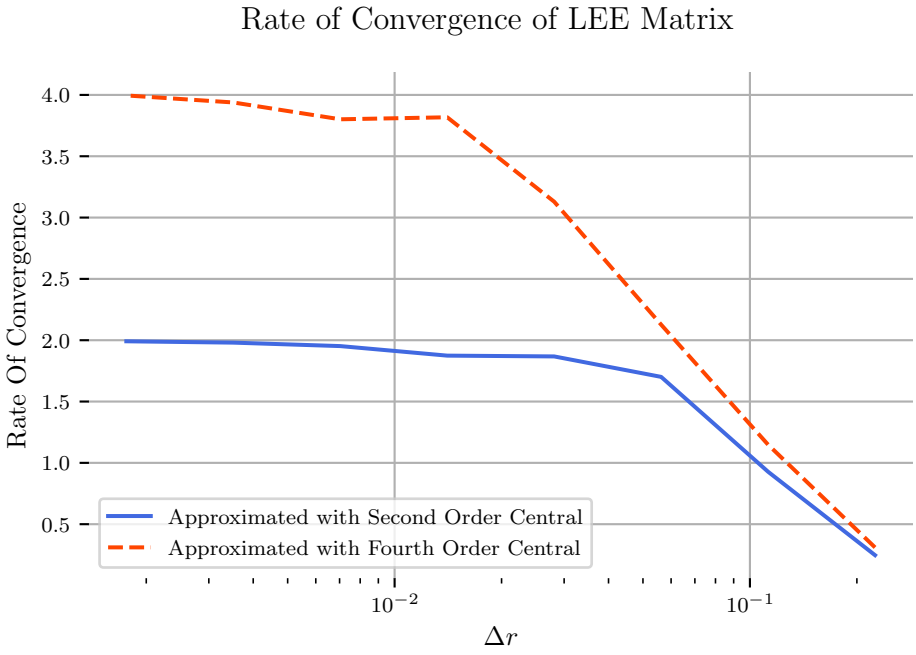
Rate of Convergence of LEE Matrix
Rate Of Convergence
4.0
3.5
3.0
2.5
2.0
1.5
1.0
0.5
Approximated with Second Order Central
Approximated with Fourth Order Central
10^{-2}
10^{-1}
Δr

References

[1] Eric W Weisstein. Bessel function of the first kind. *https://mathworld. wolfram. com/*, 2002.